Protist

ORIGINAL PAPER

Phylogenetic Position of the Parasitoid Nanoflagellate *Pirsonia* inferred from Nuclear-Encoded Small Subunit Ribosomal DNA and a Description of *Pseudopirsonia* n. gen. and *Pseudopirsonia mucosa* (Drebes) comb. nov.

Stefanie Kühn[a], Linda Medlin[b], and Gundula Eller[c,1]

[a] Department of Marine Botany (FB2), University of Bremen, Leobener Str./NW2, D-28359 Bremen
[b] Alfred Wegener Institute for Polar and Marine Research, Am Handelshafen 12, D-27570 Bremerhaven
[c] Department of Physiological Ecology, Max Planck Institute for Limnology, August-Thienemann-Strasse 2, D-24306 Plön

Sequences of the nuclear encoded small subunit (SSU) rRNA were determined for *Pirsonia diadema*, *P. guinardiae*, *P. punctigerae*, *P. verrucosa*, *P. mucosa* and three newly isolated strains 99-1, 99-2, 99-S. Based on phylogenetic analysis all *Pirsonia* strains, except *P. mucosa*, clustered together in one clade, most closely related to *Hyphochytrium catenoides* within the group of stramenopiles. However, *P. mucosa* was most closely related to *Cercomonas* sp. SIC 7235 and *Heteromita globosa* and belongs to the heterogenic group of Cercozoa. In addition to the SSU rDNA sequences, *P. mucosa* differs from the stramenopile *Pirsonia* species in some characteristics and was therefore redescribed in this paper as *Pseudopirsonia mucosa*. The three newly isolated strains 99-1, 99-2, and 99-S differed by 28 bp in their SSU rDNA sequences from their closest neighbour *P. diadema* and only 1 to 3 bp among themselves. These base differences and a host range similar to *P. formosa* were sufficient to assign them as new strains of *P. formosa*.

Introduction

Parasitoid protists are small unicellular eukaryotic heterotrophs that infect, consume and thereby inevitably kill their phytoplankton hosts. Most of the planktonic diatoms in the North Sea (53 species observed, unpublished) are susceptible to infections. These parasitoids comprise diverse taxonomic groups, such as euglenozoa, dinoflagellates, cercomonads, plasmodiophorids, oomycetes and chytrids (fungi), and species of unknown affiliation (e.g. Bulman et al. 2001; Drebes 1966; Drebes and Schnepf 1988, 1998; Kühn et al. 2000; Schnepf 1994; Schweikert and Schnepf 1996). Although host-specific parasitoids can decimate a diatom population by more than 90 per cent (Grahame 1976; Tillmann et al. 1999), their role in the marine planktonic food web is still poorly understood. Only recently, a novel flagellate, *Parvilucifera infectans*,

[1] Corresponding author;
fax 49-4522763310
e-mail eller@mpil-ploen.mpg.de

was described that kills toxic dinoflagellates (Norén et al. 1999), indicating the possible importance of parasitoids for the control of harmful algal blooms. Additionally, parasitoid nanoflagellates (PNF) often have small and flexible cells, possibly enabling them to pass through filter membranes with a poresize below the 3 μm pore that is normally used by oceanographers to fractionate water samples. This might lead to their detection in the so-called picoplanktonic fraction of the phytoplankton. PNF may therefore play an important role in the hitherto undefined heterotrophic fraction of the picoplanktonic community.

Pirsonia species are PNF that infect planktonic diatoms. Their feeding mode is unique: flagellates attach to the diatom frustule and squeeze a pseudopod into the cell, either between the girdle bands or through the rimoportulae or labiate processes, which are tubular openings that penetrate the valve wall. The pseudopod then becomes the trophosome, which phagocytises and digests the diatom protoplast. Digested material is transported into the auxosome, the part of the body that remains on the outside of the frustule. The auxosome then grows, divides and reproduces, forming offspring as long as food supply continues. Up to now, seven Pirsonia species have been described from the North Sea (Schnepf et al. 1990; Kühn et al. 1996; Schweikert and Schnepf 1997), and another 5 strains have been isolated. Ultrastructural examination clearly assigned Pirsonia to the stramenopiles (Heterokonta) (Schnepf and Schweikert 1996). Stramenopile is a term that was introduced as a rankless, informal name for eukaryotes possessing a flagellum with tripartite, tubular hair-like projections (mastigonemes) (Patterson 1989), and comprises a huge range of taxa that include parasites, saprotrophs, heterotrophs and autotrophs (e.g. brown algal kelps and diatoms).

Here we show that, based on SSU rDNA sequence analysis, the genus Pirsonia forms a distinct clade within the stramenopiles, with Hyphochytrium catenoides and Rhizidiomyces apophysatus as their next known relatives. Molecular analysis, however, shows that Pirsonia mucosa Drebes does not belong to the stramenopiles but is related to the cercomonads. Furthermore, we describe a new genus, Pseudopirsonia gen. nov., for this taxon.

Results

Morphology and host range

The life cycle of all Pirsonia species and Pseudopirsonia is similar (Fig. 1) (Kühn 1996). As soon as phagocytosis begins the diatom protoplast structure becomes notably affected (Fig. 2A). Non-particulate nutrients are transported into the main body of the former flagellate, which remains outside the frustule and becomes the auxosome (Fig. 2B, 2C). Trophosomes of adjacent auxosomes frequently fuse. As long as nutrients are transported into the auxosomes these continue to grow and divide. The offspring eventually grow flagella and become infective flagellates.

Five Pirsonia species were described in detail by Kühn et al. (1996). In this study, we included three newly isolated strains Pirsonia 99-1, 99-2 and 99-S, which were assigned to P. formosa as described below. Pirsonia species differ only slightly in their morphological characteristics (Table 1). The flagellate of P. verrucosa is, for example, approximately 8 μm long and 3 μm wide, and thereby slightly smaller than the flagellate of the new Pirsonia formosa 99-S with 9-13 × 6 μm. The anterior flagellum measures in all species 15 to 25 μm, but the length of the posterior flagellum is variable with 15 μm in P. verrucosa and 45 μm in P. eucampiae. Additional morphological features like the size and shape of the auxosomes, or whether flagellate mother cells remain connected to the diatom frustule show only minor differences for the hitherto identified species. Cyst formation was only observed for P. guinardiae and P. formosa 99-2. Hatching was never observed.

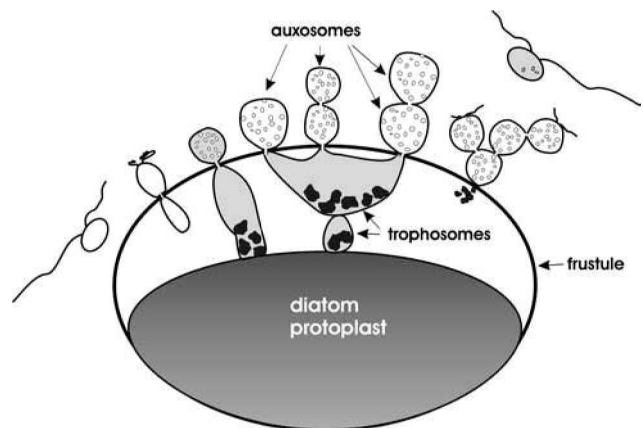**Figure 1.** Developmental stages of Pirsonia and Pseudopirsonia. Motile flagellates attach and penetrate frustule with a pseudopod. The pseudopod phagocytises and digests portions of the diatom protoplast and thus differentiates into the trophosome. Nutrients are transported into the body of the former flagellate, now called auxosome. The auxosome grows and divides, forming offspring as long as trophosomes continue to phagocytise.

A characteristic feature for the *Pirsonia* species is their host range (Table 2). Some species, e.g. *P. diadema* and *P. punctigerae,* are host specific and infect only one diatom genus whereas the host range of the newly isolated *Pirsonia formosa* strains 99-1, 99-2 and 99-S is relatively broad and similar to that of *P. formosa*. Circumstantial evidence indicates that there might be a transition between an initial chemosensory attraction and possibly successful infection by later parasitoid generations. *Pirsonia*

formosa 99-1 was attracted to *Stephanopyxis turris* and attached to the frustule but failed to penetrate (not shown). *Pirsonia formosa* 99-2 was clearly chemosensory attracted to *Thalassiosira punctigera,* but did not attach to the frustule (Fig. 2D), even though it attached to the diatom protoplast (Fig. 2E). *Pirsonia formosa* 99-S was strongly attracted by *Guinardia flaccida* and attached to the frustule (Fig. 2F). Successful infections, however, were scarce.
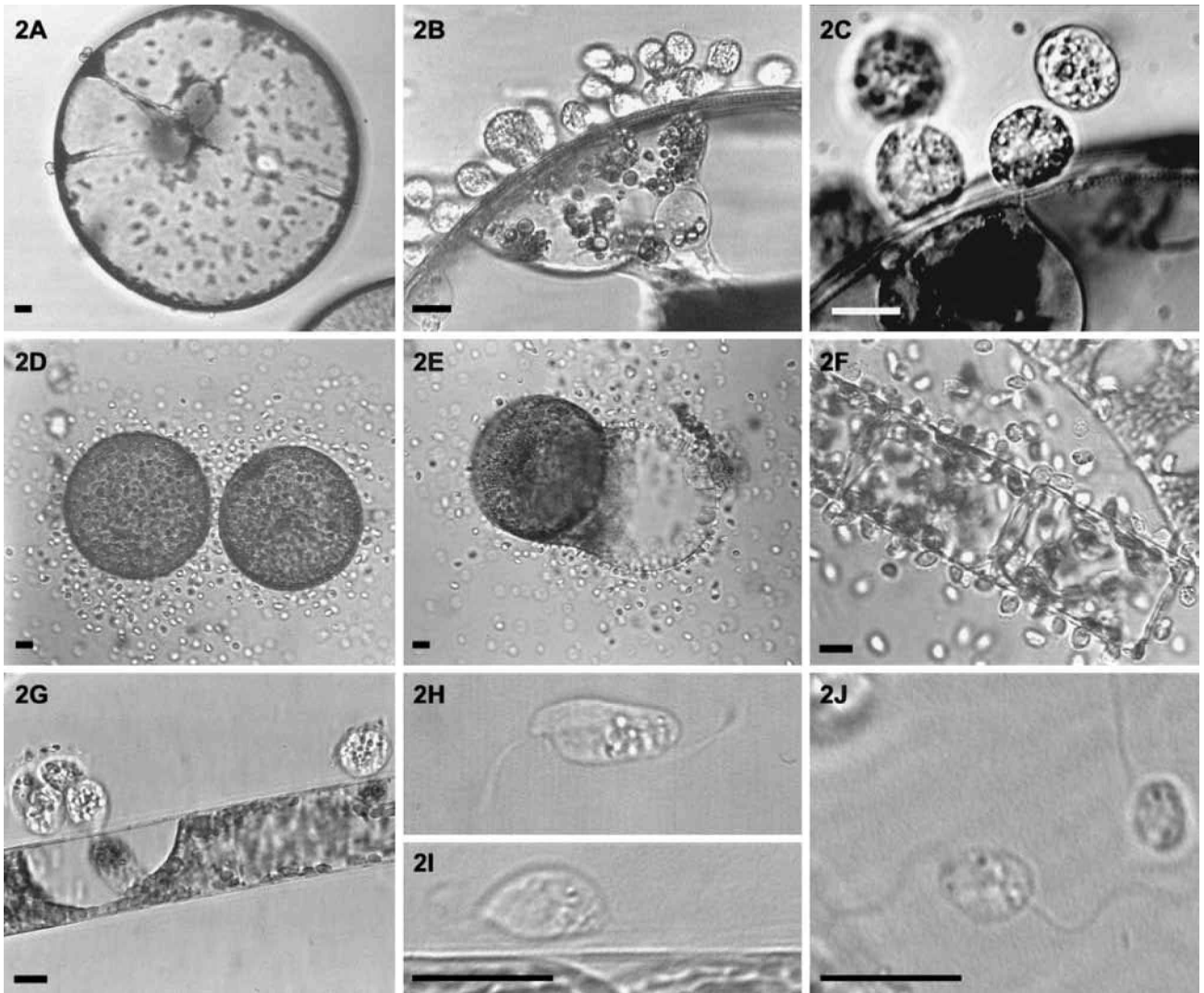
Figure 2. *Pirsonia* species and *Pseudopirsonia mucosa*. **A–C.** *Pirsonia diadema* infecting the marine diatom *Coscinodiscus wailesii*. **A.** Infection after approximatly 6 hours at room temperature. **B.** *P. diadema*, auxosomes and trophosomes. **C.** *P. diadema*, detail of cytoplasmatic connection between divided auxosomes. **D.** *P. formosa* 99-2 flagellates are clearly chemosensory attracted by *Thalassiosira punctigera* but do not attach to the diatom frustule. **E.** *P. formosa* 99-2 flagellates attach to the naked protoplast of *T. punctigera*. **F.** *P. formosa* 99-S attach to *Guinardia flaccida* but only succeed occassionally to infect the diatom. **G–I.** *Pseudopirsonia mucosa*. **G.** Auxosomes with mucilagenous coat and adhering bacteria and trophosomes (feeding on *Rhizosolenia imbricata*). **H.** Flagellate, dorsal view. **I.** Flagellate, lateral view. **J.** *Pirsonia diadema* flagellates. (Bars = 10 μm.)

Phylogenetic Analysis

Full length sequences of the nuclear encoded SSU rRNA gene were determined for *Pirsonia diadema*, *P. guinardiae*, *P. punctigerae, P. verrucosa*, *Pirsonia formosa* strains 99-1, 99-2 and 99-S and *Pseudopir-* *sonia mucosa*. All methods used for phylogenetic analysis placed the *Pirsonia* spp. next to *Hyphochytrium catenoides* (accession numbers X80344 and AF163294) and *Rhizidiomyces apophysatus* (accession number AF163295) within the group of stramenopiles (Fig. 3A). In contrast to

Table 1. Morphological characteristics of several *Pirsonia* species.

Pirsonia/ Pseudopirsonia	Size of flagellates (µm)	Length of anterior and posterior flagellum (µm)	Retraction of flagella after infection	Shape of primary auxosomes	Size of primary auxosomes (µm)	Cysts
P. diadema	8–10 × 3–4	16–18, 35–40	early	apple-shaped	10	–
P. eucampiae	7–9 × 4–5	15, 45	never completely	globular	12	–
P. formosa	7–8 × 5–6	18, 25–30	early	globular	13	–
P. formosa 99-1	9 × 5	18–22, 20–24	early	apple-shaped	10 × 12	–
P. formosa 99-2	6–8 × 3–4	12–14, 17–19	early	globular	10	+
P. formosa 99-S	9–13 × 6	16–20, 22–25	never completely	apple-shaped to globular	10 × 11	–
P. guinardiae	10 × 6	15, 25	never completely	apple-shaped	15	+
P. punctigerae	7–8 × 3–4	20–25, 25–30	very early	apple-shaped	12	–
P. verrucosa	8 × 3	10, 15	very late	apple-shaped	12	–
Pseudopirsonia mucosa	12–14 × 5–7	20–25, 25–30	early	globular	18	

Table 2. Diatom host range of *Pirsonia* species.

Pirsonia/ Pseudopirsonia Diatom	*P. diadema*	*P. eucampiae*	*P. formosa*	*P. formosa* 99-1	*P. formosa* 99-2	*P. formosa* 99-S	*P. guinardiae*	*P. punctigerae*	*P. verrucosa*	*Pseudopirsonia mucosa*
Cerataulina pelagica	—	+	HP				—		—	HR/—
Coscinodiscus concinnus	+	—	—				—			—
C. granii	HP	—	○			—	—	—	—	—
C. wailesii	HP	—	—				—	—	—	—
Eucampia zodiacus	—	HP	++	++	HP	—	—		—	
Guinardia delicatula	—	—	++	++	HR	HP	+	—	HP	+
G. flaccida	—	—	+	++	(+)	(+)	HP	—	—	+/○
Leptocylindrus danicus	—	–	HP	HP	++	—	—		—	+
Rhizosolenia imbricata	—	—	HP	++	++	+	—			HP
R. setigera	—	—	HP				—	—	—	+
R. similoides				++	++	(+)				
Stephanopyxis turris	—		(+)	○	—	○	—			—
Thalassiosira punctigera	—	—	—	○	—	○	—	HP		—
T. rotula	—	—	—	○	—	—	—	+	—	—

HP, host in plankton; HR, host in raw cultures (growth medium added to plankton sample); ++, very rapid infection; +, good infection; (+), hesitant infection; ○, attachment but no feeding; –, no infection in plankton samples; —, no infection in laboratory host range studies.

Table 3. List of possible probe sequences for the genus *Pirsonia* as designed in ARB. Only probe Pirsonia B was tested in dot blot hybridisations. Given are the probe and selected non-target sequences, illustrating the position of mismatches.

Probe Name	E-coli Position	Tm (GC+AT) *Number of sequences with given mismatch*	**Probe sequence 5′-3′** Target sequence 3′-5′ – mismatches in non-targets –
Pirsonia A	1100	58 °C	**5′-GCGGTCGTCTCGTTCGTT-3′** 3′-CGCCAGCAGAGCAAGCAA-5′
		> 50 sequ	3′-====GC============-5′
		> 60 sequ	——-====CC============——
Pirsonia B	1134	60 °C	**5′-CCCGCCAACGCAAGCGTT-3′** 3′-GGGCGGTTGCGTTCGCAA-5′
		1 sequ	——-==C====G========C=——
		1 sequ	——-C===========AA===——
		4 sequ	——-N=====A=====G==A==——
		2 sequ	——-======GC======TC=——
		> 70 sequ	——-=====A=====GA=A==——
Pirsonia C	183	58 °C	**5′-CCTTCCGCACAGGCAGTT-3′** 3′-GGAAGGCGTGTCCGTCAA-5′
		3 sequ	——-==C=====C==T======——
		9 sequ	——-==C=====GC=======——
		2 sequ	——-==CG====C==T======——
		> 20 sequ	——-==C=====GC=T======——
Pirsonia E	1159	56 °C	**5′-CCCTGATTAGTCACCAGG-3′** 3′-GAAGGGGACTAATCAGTG-5′
		4 sequ	——-=A===C===========T——
		1 sequ	——-========TT==A====——
		4 sequ	——-========GAG=C=====——
Pirsonia I	632	54 °C	**5′-GCAAGAGACGACACTAGT-3′** 3′-CGTTCTCTGCTGTGATCA-5′
		8 sequ	——-==G======T===T===——
		4 sequ	——-==G======T===C===——
		2 sequ	——-==G=G========T===——
		2 sequ	——-==GC=======C=====——

this, *Pseudopirsonia mucosa* Drebes is most closely related to the cercomonads *Cercomonas* sp. SIC 7235 (accession number AF277495) and *Heteromita globosa* (accession number U42447, Fig. 3B).
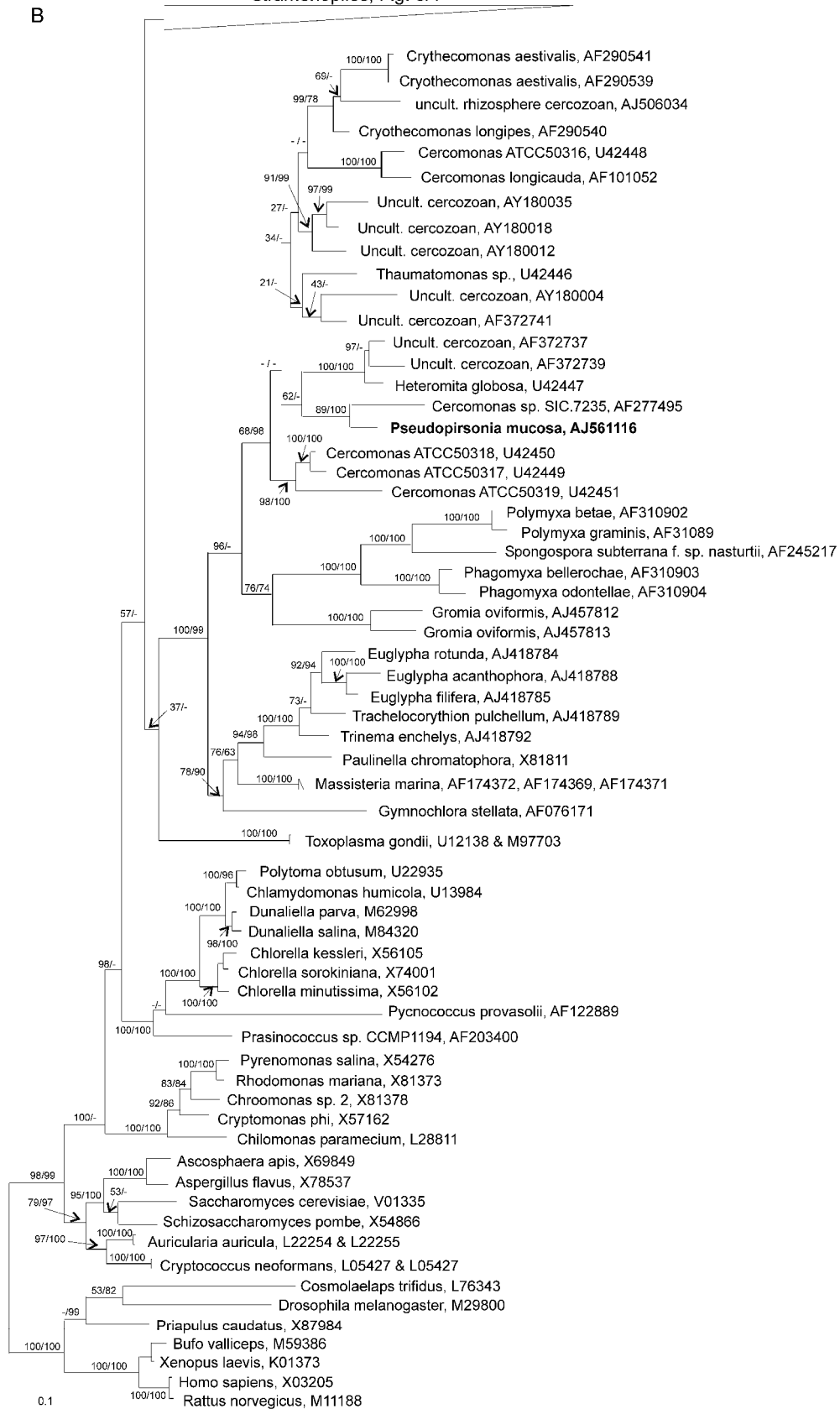
The dendograms calculated using the Maximum Likelihood (ML), Neighbour Joining (NJ) and Maximum Parsimony (MP) methods varied inside the stramenopile or cercomonade groups in some branching positions. Nevertheless, the relative position of all *Pirsonia* sequences to their closest relatives was stable, albeit with low bootstrap support

(Fig. 3A). Bootstrap values for these relationships were 48/96 for the clade of *Pirsonia* spp. and *Hyphochytrium/Rhizidiomyces* and 89/100 for the *Pseudopirsonia/Cercomonas* SIC clade as calculated by MP and NJ analysis with 1000 replicates, respectively. The *Pirsonia* species belonging to the stramenopiles clustered closely together, showing only 0.2–2.4% dissimilarity in the distance matrix. *Hyphochytrium catenoides* had dissimilarities of 7.0–7.9% to these *Pirsonia* sequences. The dissimilarity of *Pseudopirsonia mucosa* to the stramenopile

Figure 3. Phylogenetic position of *Pirsonia* and *Pseudopirsonia* among eukaryotes. Dendogram calculated with 162 sequences using ML algorithm and a 50% base frequency filter for the *Pirsonia* and *Pseudopirsonia* sequences. For a better graphical resolution, the tree was graphically divided into two partial figures. **A.** Stra-

B

Stramenopiles, Fig. 3A


```
                                    100/100  ┌─ Crythecomonas aestivalis, AF290541
                              69/-  ┌─────────┤
                                    │         └─ Cryothecomonas aestivalis, AF290539
                        99/78 ┌─────┤
                              │     └─────────── uncult. rhizosphere cercozoan, AJ506034
                        ┌─────┤
                        │     └─────────────── Cryothecomonas longipes, AF290540
                  - / - │            100/100  ┌─ Cercomonas ATCC50316, U42448
                        │     ┌───────────────┤
                  91/99 │     │               └─ Cercomonas longicauda, AF101052
                  ┌─────┤ 97/99│
                  │     27/-  └── Uncult. cercozoan, AY180035
                  │  ┌──┤
                  │  │  └────────── Uncult. cercozoan, AY180018
                  │34/-
                  │  └──────────── Uncult. cercozoan, AY180012
                21/-        ┌── Thaumatomonas sp., U42446
                  │   43/- ┌─┤
                  └────────┤ └── Uncult. cercozoan, AY180004
                           └──── Uncult. cercozoan, AF372741
```

97/- Uncult. cercozoan, AF372737
100/100 Uncult. cercozoan, AF372739
- / - Heteromita globosa, U42447
62/- 89/100 Cercomonas sp. SIC.7235, AF277495
68/98 **Pseudopirsonia mucosa, AJ561116**
100/100 Cercomonas ATCC50318, U42450
Cercomonas ATCC50317, U42449
98/100 Cercomonas ATCC50319, U42451

96/- 100/100 Polymyxa betae, AF310902
100/100 Polymyxa graminis, AF31089
Spongospora subterrana f. sp. nasturtii, AF245217
100/100 100/100 Phagomyxa bellerochae, AF310903
76/74 Phagomyxa odontellae, AF310904
100/100 Gromia oviformis, AJ457812
Gromia oviformis, AJ457813
92/94 100/100 Euglypha rotunda, AJ418784
Euglypha acanthophora, AJ418788
73/- Euglypha filifera, AJ418785
100/100 Trachelocorython pulchellum, AJ418789
94/98 Trinema enchelys, AJ418792
76/63 Paulinella chromatophora, X81811
78/90 100/100 Massisteria marina, AF174372, AF174369, AF174371
Gymnochlora stellata, AF076171

57/- 100/99 37/-

100/100 Toxoplasma gondii, U12138 & M97703

100/96 Polytoma obtusum, U22935
Chlamydomonas humicola, U13984
100/100 Dunaliella parva, M62998
100/100 Dunaliella salina, M84320
98/100 Chlorella kessleri, X56105
100/100 Chlorella sorokiniana, X74001
Chlorella minutissima, X56102
98/- -/- 100/100 Pycnococcus provasolii, AF122889
100/100 Prasinococcus sp. CCMP1194, AF203400

100/100 Pyrenomonas salina, X54276
83/84 Rhodomonas mariana, X81373
92/86 Chroomonas sp. 2, X81378
Cryptomonas phi, X57162
100/- 100/100 Chilomonas paramecium, L28811

100/100 Ascosphaera apis, X69849
98/99 Aspergillus flavus, X78537
95/100 53/- Saccharomyces cerevisiae, V01335
79/97 Schizosaccharomyces pombe, X54866
97/100 100/100 Auricularia auricula, L22254 & L22255
100/100 Cryptococcus neoformans, L05427 & L05427

53/82 Cosmolaelaps trifidus, L76343
-/99 Drosophila melanogaster, M29800
100/100 Priapulus caudatus, X87984
100/100 Bufo valliceps, M59386
Xenopus laevis, K01373
100/100 Homo sapiens, X03205
0.1 100/100 Rattus norvegicus, M11188

menopile sequences. **B.** Cercozoa and outgroup sequences. Numbers are bootstrap values for the MP/NJ analysis, each with 1000 replicates. In the ML analysis, only the branches marked with * were not significantly positive (P > 0.05, 72004 trees calculated).
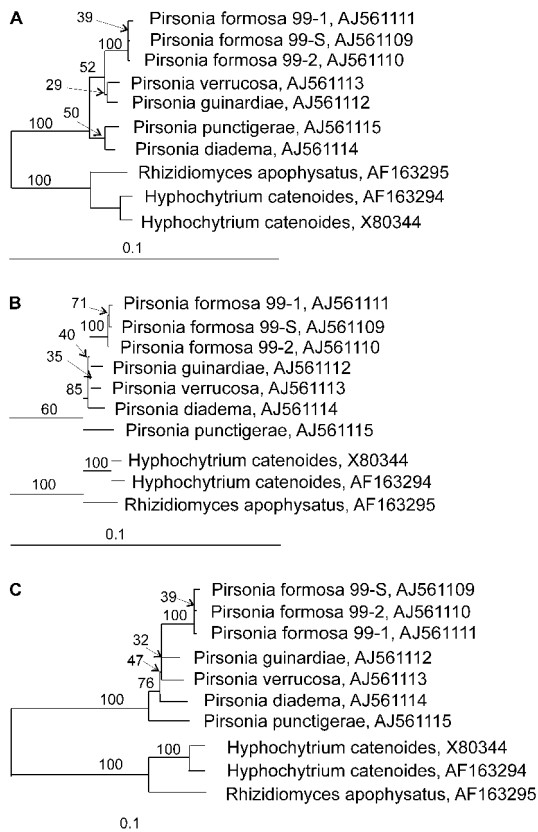
A

```
        39 ┐┌ Pirsonia formosa 99-1, AJ561111
       100 ├ Pirsonia formosa 99-S, AJ561109
        52 │└ Pirsonia formosa 99-2, AJ561110
        29 ┐┌ Pirsonia verrucosa, AJ561113
        50 └ Pirsonia guinardiae, AJ561112
   100 ┌ Pirsonia punctigerae, AJ561115
       └ Pirsonia diadema, AJ561114
 100 ┌ Rhizidiomyces apophysatus, AF163295
     └┌ Hypochytrium catenoides, AF163294
      └ Hypochytrium catenoides, X80344
              0.1
```

B

```
        71 ┐┌ Pirsonia formosa 99-1, AJ561111
     40 100 ├ Pirsonia formosa 99-S, AJ561109
        35 └ Pirsonia formosa 99-2, AJ561110
           Pirsonia guinardiae, AJ561112
        85 ┐ Pirsonia verrucosa, AJ561113
        60 └ Pirsonia diadema, AJ561114
           Pirsonia punctigerae, AJ561115
       100 ┐ Hypochytrium catenoides, X80344
   100 └ Hypochytrium catenoides, AF163294
       Rhizidiomyces apophysatus, AF163295
              0.1
```

C

```
        39 ┐┌ Pirsonia formosa 99-S, AJ561109
       100 ├ Pirsonia formosa 99-2, AJ561110
        32 └ Pirsonia formosa 99-1, AJ561111
        47 ┐ Pirsonia guinardiae, AJ561112
        76 └ Pirsonia verrucosa, AJ561113
   100 ┌ Pirsonia diadema, AJ561114
       └ Pirsonia punctigerae, AJ561115
       100 ┌ Hypochytrium catenoides, X80344
   100 └ Hypochytrium catenoides, AF163294
       Rhizidiomyces apophysatus, AF163295
              0.1
```

Figure 4. The branching order among the *Pirsonia*. All calculations were carried out with the 10 sequences shown in the figures, using all unambiguously aligned positions (1835 valid columns). For all algorithms a bootstrap analysis with 1000 replicates was carried out. **A.** The *Pirsonia* clade as calculated by ML. **B.** The *Pirsonia* clade as calculated by NJ. **C.** The *Pirsonia* clade as calculated by MP.

Pirsonia clade was with 17.9–19.2% high, and even the closest relative in the trees, *Cercomonas* SIC, showed 9.2% dissimilarity. The branching order inside the *Pirsonia* clade, calculated with only 10 sequences and using all unambiguously aligned positions, differed slightly with the different methods used for calculation, except that the new strains (*P. formosa*) are last to diverge (Fig. 4). *Pirsonia guinardiae* and *P. verrucosa* form a sister group in the NJ and ML analysis, but not in the tree calculated with MP. Additionally, the relative position of *P. punctigerae* within the *Pirsonia* clade changed, forming a sister group with *P. diadema* only in the ML analysis. Therefore, in Figure 3A the *Pirsonia* clade is given as consensus of all dendograms generated with the different algorithms.

Due to the complicated cultivation and maintenance of parasitoid cultures, the loss of described

type species is possible, and already happened for the *Pirsonia formosa* type strain. To make the re-detection of these species in environmental samples and/or cultures easier, we designed oligonucleotide probes for the genus *Pirsonia*. Several oligonucleotide sequences with 0 mismatches to the genus *Pirsonia* and at least 2 mismatches to non-target sequences were developed (Table 3). Probe Pirsonia B reacted specifically with the rDNA of all 7 *Pirsonia* species in dot blot hybridisations at a hybridisation temperature of 63 °C and 0.5 × SSC as washing buffer. As intended by the probe design, *Pseudopirsonia mucosa* was not detected with this probe.

Discussion

The SSU rDNA sequences of all the known *Pirsonia* species (with the exception of *Pseudopirsonia mucosa*) form a distinct phylogenetic clade, with *Hyphochytrium catenoides* as its sister group. However, concerning life cycle and diet, *Pirsonia* and *Hyphochytrium* show major differences. *H. catenoides* (phylum Hyphochytriomycota), is a heterotrophic organism, which lives parasitically or saprophytically in freshwater algae and even on *Zea mays*. Its life cycle includes the formation of zoospores with only one, anterior flagellum, bearing tripartite hairs (or mastigonemes). These zoospores show encystment, germinate and form an eucarpic, polycentric thallus that acquires nutrients by absorption (Sparrow 1960; Fuller 1990). In contrast to this, in *Pirsonia* the flagellates acquire nutrients by phagocytosis of the diatom protoplast. Encystment has only occassionally been observed in two species (*P. guinardiae*, *P. formosa* 99-2).

Stramenopile *Pirsonia* differ morphologically from their closest relative

In addition to a different lifestyle, the comparison of the ultrastructure of *Pirsonia* and *H. catenoides* showed prominent differences. The most important is the aggregation of ribosomes in an area next to the nucleus in *H. catenoides*, which is missing in *Pirsonia* (Cooney et al. 1985; Schnepf and Schweikert 1996). Moreover, the nucleus in *Pirsonia* is rounded and euchromatic, whereas it is elongated and strongly heterochromatic in *H. catenoides*. In contrast to *H. catenoides*, the mitochondria of *Pirsonia* have regularly arranged parallel tubular cristae. Additionally, *Pirsonia* has several small or large lipid droplets, depending on the nutritional status of the flagellates, scattered among the cell body. *H. catenoides* has only one large lipid body, predomi-

nantly at the posterior region of the cell. The kinetosome of the anterior flagellum has in both organisms one rootlet that consists of a fibrillar-microtubule with electron-opaque material attached to one side. In *H. catenoides*, the other rootlet consists of a pair of microtubules and bears four rib microtubules, whereas in *Pirsonia* it consists of four microtubules. The transition zone, however, is very similar in both organisms and is a construction that is characteristic for the stramenopiles. In both organisms bulges on the anterior end of the nucleus are in close contact to the flagellar root apparatus.

These differences in ultrastructure and life cycle of the two genera support the importance of the sequence dissimilarities detected by phylogenetic analysis. Even the closely related *Hyphochytrium* was shown to differ in major characteristics from *Pirsonia*. Cavalier-Smith (1998) erected a new order Pirsoniales and a new class Pirsoniaceae within the phylum Sagenista, subphylum Bicoecia, which also includes the heterotrophic flagellate *Cafeteria*. We show, however, that a considerable phylogenetic distance separates *Pirsonia* from *Cafeteria* (Fig. 3A).

Pirsonia versus *Pseudopirsonia*

In contrast to the *Pirsonia* spp. described above, *Pseudopirsonia mucosa* Drebes (*Pirsonia mucosa* Drebes, Kühn et al. 1996) is related to the cercomonads, a group of morphologically diverse amoeboflagellates, and not to the stramenopiles. In order to distinguish this parasitoid nanoflagellate from *Pirsonia* we redescribe it as *Pseudopirsonia mucosa*. It differs from *Pirsonia* in several morphological characteristics. The body of *P. mucosa* has an oval-oblong shape with an apical "nose", and the size of mature flagellates is 5–7 × 12–14 μm (Fig. 2H, I), whereas *Pirsonia* spp. have a rounded to oval cell shape and a cell size in the range of 4–7 × 7–12 μm (Fig. 2J). In *P. mucosa* the flagella are inserted in median position or even submedianly in contrast to *Pirsonia* spp., where they are subapically inserted on the ventral side. Additionally, in *P. mucosa* the dividing auxosomes are morula-shaped and covered by a mucilaginous coat where bacteria frequently attach (Fig. 2H). In *Pirsonia* spp. offspring developing from auxosomes never form a globular aggregation. Moreover, the attacking flagellates of *P. mucosa* attach to the diatom frustule with a broad pseudopod that emerges laterally, whereas in *Pirsonia* spp. flagellates attach with a posteriorly protruded pseudopod. Another characteristic is the rather slow gliding movement of the *P. mucosa* flagellates compared to the slightly jerking swimming movements of *Pirsonia* spp.. Important similarities between *Pirsonia* and *Pseudopirsonia* are the life cycles, which include the formation of conspicuous trophosomes and auxosomes.

The comparison of *Pseudopirsonia* with the cercomonads revealed differences in their use of the pseudopod. The pseudopod of *Pseudopirsonia* differentiates into a trophosome soon after the beginning of phagocytosis on the diatom protoplast. In contrast to this, other cercomonads use the pseudopod to take up food particles, which are then digested in food vacuoles inside their own body (Karpov 1997; Macdonald et al. 1977; Schnepf and Kühn 2000; Thomsen et al. 1990). Because *P. mucosa* has not yet been studied ultrastructurally we cannot confirm its molecular relatedness to *Heteromita globosa* or other cercomonads with synapomorhies in the flagellates structure and organization.

Host range, speciation and sequence similarities

It has been suggested that host specificity evolved from a broader host range to a narrower one. Phylogenetic analysis of the parasitoid nanoflagellate *Cryothecomonas* indicated that *C. longipes* with the broadest host range (at least 14 diatom species) diverged prior to the separation of the two strains of *C. aestivalis,* which infects only one, respectively two diatom species of the same genus (Kühn et al. 2000). A correlation between host range and sequence similarities was also found for two species of the diatom parasitoid *Phagomyxa*. These *Phagomyxa* species were isolated from different host genera (*Bellerochea* and *Odontella*) and showed significant differences in their 18S rDNA sequences (Bulman et al. 2001). Comparable results were reported for the marine parasitic dinoflagellate *Amoebophrya ceratii* (Koeppen) Cachon, an obligate parasite of other dinoflagellates. These parasites show genetic divergence among strains, which infect different hosts (Coats and Park 2002; Gunderson et al. 2002; Janson et al. 2000).

The identification of the phytoplankton host appears to be a reliable indicator of *Pirsonia* speciation as differences in nucleotides among parasitoids appear to reflect differences in their host ranges. *P. diadema*, which infects only the diatom genus *Coscinodiscus*, differs 28 nucleotides over the total sequence length from the three new *Pirsonia formosa* strains. These, on the other hand, have a very similar host range to that of *P. formosa* and differ only in one to three nucleotides from one another. We therefore consider them as strains of *P. formosa,* although the type strain of this species was no longer available for sequencing.

Phylogenetic analysis based on all unambiguously aligned positions of *Pirsonia* shows that *P. guinardiae* and *P. verrucosa* are closely related (Fig. 4). Additionally, they have a similar host range, infecting only diatoms of the genus *Guinardia* (Table 2). However, the phylogenetic analysis gives the impression that host specificity is not always supported by sequence data: Depending on the analytical method, *P. punctigerae* and *P. diadema* are either branching together (ML, Fig. 4A) or are separated from other *Pirsonia* species (NJ, MP Fig. 4B, C) even though they infect only one diatom species (Table 2). The important difference, which might explain the branching instability is the way of host infection. Usually, *Pirsonia* species infect their hosts in the girdle region of the frustule, but *P. diadema* and *P. punctigerae* infect their hosts solely by penetrating pores in the valves (rimoportulae in *Coscinodiscus* and fultoportulae in *Thalassiosira*). Nevertheless, our study with 18S rDNA sequences of *Pirsonia* does not support the assumption that evolution shapes towards host specificity, as *P. formosa* with the broadest host range diverged last in the genus. This evolutional hypothesis has to be confirmed by analysis of the variable region of the large subunit rRNA, which should include more differences between the individual *Pirsonia* sp. and thereby allow a deeper branching inside the clade (work in progress).

Explanation for the occurrence of *Pirsonia* in picoplanktonic clone libraries

Taxonomically identified species in sister groups of *Pirsonia*, such as *Hyphochytrium catenoides* (Hyphochytiomycetes), *Developayella elegans* (unassigned), the oomycetes *Lagenidium gigantum*, *Achlya bisexualis*, *Phytophtora megaspermum* and the labyrinthulids *Thraustochytrium kinnei*, *Labyrinthuloides haliotidis*, *Ulkenia profunda* are parasitic or saprophytic. Other sequences related to *Pirsonia* belong to not yet isolated and identified eukaryotic picoplanktonic stramenopiles, which were obtained from clone libraries (Díez et al. 2001; Massana et al. 2002; Moon-van der Staay et al. 2001). The assignment of these sequences to the picoplankton was based on the filtration of plankton samples through filter membranes with a pore size of 3 µm and the set up of the clone libraries with the filtrate. Because heterotrophic nanoflagellates even slip through very small pore sizes of 0.8 µm (Beardsley 2003) it is very likely that *Pirsonia* and *Pseudopirsonia* flagellates with their soft cell structure will be found in filtrates from 3 µm pore size filters. The relation of the novel picoplanktonic sequences to parasitic and saprophytic groups suggests that they also could be parasitoids, parasites or saprophytes. A parasitic nature of these organisms would also explain the failure to cultivate them with the methods for heterotrophic and phototrophic growth described by the authors (Massana et al. 2002).

Conclusions

Our phylogenetic analysis showed that species described as *Pirsonia* were not monophyletic: (i) one group of *Pirsonia* spp. clusters within the group of stramenopiles and includes *P. verrucosa*, *P. diadema*, *P. formosa*, *P. guinardiae*, *P. punctigerae*, whereas (ii) *P. mucosa* clusters within the heterogenous group of cercozoa with *Cercomonas* SIC as its closest relative. Consequently, *P. mucosa* was moved to a new genus *Pseudopirsonia* based on these results and additional morphological characteristics. The ecological relevance of these parasitoids will be determined using the specific oligonucleotide probe developed based on results described here (work in progress).

Taxonomic appendix

Our taxonomic decisions are placed in the context of the higher level classification available via micro*scope: http://www.mbl.edu/microscope

Eucaryote
Cercomonadidae
Cercomonadida incertae sedis

Pseudopirsonia Kühn Medlin & Eller new genus: Obligate parasitoid nanoflagellate that preys on marine diatoms. Cell with apical "nose", two medially inserted flagella; feeds by means of a trophosome; dividing auxosomes are globular and covered by a mucilaginous coat, frequently with adhering bacteria; movement gliding rather than swimming, feeds on the diatoms *Rhizosolenia imbricata*, *R. setigera*, *Leptocylindrus danicus*, *Guinardia delicatula* and *G. flaccida*.

With one species: *Pseudopirsonia mucosa* (Drebes) Kühn & Eller, comb. nov.

Basionym: *Pirsonia mucosa* DREBES 1996, Helgoländer Meeresunters 50; P. 219, Figure 6.

Methods

Materials: *Pirsonia* species were isolated from plankton samples collected with a 20 or 80 µm mesh

plankton net off List/Sylt in the German Wadden Sea or off Helgoland (North Sea) over a period of 7 years. Cultures were established by isolating diatoms infected by *Pirsonia*. The isolation of infected cells was carried out using a mouth pipette. Each parasitoid strain was maintained in culture with its respective diatom host(s). A few µl of infected cultures were transferred into new host cultures when most diatoms were infected. Three *Pirsonia* strains (99-1, 99-2, 99-S), described here as *P. formosa*, were isolated in September 1999 off List/Sylt and maintained with *Guinardia delicatula* as host. All *Pirsonia* species that are cultivated, currently *P. formosa* and *P. diadema*, and the DNA preparations of all species investigated can be obtained from Stefanie Kühn, University of Bremen.

DNA extraction: Parasitoids were harvested by centrifugation after all diatom cells in the culture were infected and their protoplasts consumed. This late stage of infection was chosen to prevent contamination of the parasitoid DNA preparation with diatom DNA. The culture pellets were used directly for DNA extraction. Total DNA was obtained using 3% CTAB (hexadecyl-trimethyl-ammonium-bromide) procedure as described by Doyle and Doyle (1990). Cells were lysed in 3% CTAB buffer at 60 °C for 1 h. DNA was purified by subsequent extraction with phenol/chloroform/isoamylalcohol (PCI) and chloroform/isoamylalcohol (CI). DNA was precipitated with isopropanol and the pellet washed with ethanol. After resuspension in PCR grade water, RNA and proteins were removed (Rnase and Proteinase K treatment), proteins extracted again with PCI and CI and DNA precipitated with 100% ethanol. Finally, DNA was resuspended in pH stabilized PCR grade water and concentration estimated photometrically by measuring the adsorption at 260 nm.

PCR amplification: The SSU rRNA genes of the parasitoids were amplified using the universal eukaryotic primers 1F (5′- AAC CTG GTT GAT CCT GCC AGT A-3′) and 1528R (5′-GAT CCT TCT GCA GGT TCA CCT AC-3′) as described by Medlin et al. (1988). Each 100 µl PCR reaction contained 10 µl of 10× reaction buffer (100 mM Tris (pH 8.4), 500 mM KCl, 20 mM $MgCl_2$, 0.1% gelatine), 0.1 mM of each dNTP, 0.1 µM of each primer, and 2.5 to 5 units of Ampli-Taq DNA polymerase (Perkin-Elmer, Roche Molecular Systems, USA). Two different cycling protocols were followed. In the first protocol, PCR reactions were performed with hot start, using a Perkin-Elmer-Cetus thermocycler. After the initial denaturation at 95 °C for 6 min, the Taq polymerase was added to the reaction mix. The cycler cooled to 60 °C, followed by 29 cycles of 72 °C for 4 min,

94 °C for 2 min, 45 °C for 2 min, and a final extension step 72 °C for 9 min. For the second protocol, PCR reactions were prepared including the Taq polymerase and cooled on ice until placed in an Eppendorf Mastercycler Gradient (Eppendorf, Germany), with the block preheated to 94 °C (lid 105 °C). After the initial denaturation (94 °C, 5 min), 30 cycles of 94 °C for 2 min, annealing at 56 °C for 2 min and elongation at 72 °C for 4 min were carried out, followed by a final extension at 72 °C for 10 min and cooling to 4 °C. Amplification products were checked for appropriate length and purity by agarose gel electrophoresis and the template concentration varied until sharp single bands were achieved for each DNA. Both amplification protocols resulted in high quality PCR products.

Sequencing: PCR products were purified using the QIAQuick PCR purification or the MiniElute Kit (QIAGEN, Germany) following the instructions of the manufacturer. Sequencing reactions were performed following two different methods. First, the Sequi-Therm-Cycle Sequencing kit from BIOZYM (Germany) was used, with up to 200 ng template per reaction and following the instructions of the manufacturer. Sequencing reactions were run on an automated Licor sequencer (MWG, Ebersberg, Germany). For the second protocol, the Big Dye Terminator Ready Reaction Mix (BigDye v.3.0, Applied Biosystems) was used, following the instructions of the manufacturer. Approximately 10 ng template were added to each reaction mix and the annealing temperature was set to 50 °C for all primers used. Sequences were determined with a capillary sequencer (ABI Prism 3100 Genetic Analyzer, Applied Biosystems). To achieve full length double strand reads of the SSU rDNA, primers 528F (5′-GCG-GTAATTCCAGCTCCAA-3′), 1055F (5′-GGTGGTG-CATGGCCGTTCTT-3′), 536R (5′-AATTACCGCG-GCKGCTGG CA-3′), and 1055R (5′-ACGGCCATG-CACCACCACCCAT-3′) were used in addition to the primer set 1F/1528R. All sequence outputs were checked manually and consensus sequences calculated using different software packages (DNAMAN, BioEdit (Hall 1999), SeqMan (DNA-Star, Lasergene)).

Nucleotide Accession Numbers: The *Pirsonia* SSU rDNA sequences have the accession numbers AJ561109 to AJ561115, the *Pseudopirsonia* SSU rDNA sequences has the accession number AJ561116.

Phylogenetic analysis: *Pirsonia* and *Pseudopirsonia* sequences were checked for closest relatives in GenBank by BLAST Search (http://www.ncbi.nlm.nih.gov/BLAST). For phylogenetic analysis *Pirsonia* and *Pseudopirsonia* sequences and sequences of their closest relatives

found in GenBank were imported into a dataset of small subunit rDNA sequences using the ARB software package (Ludwig et al. 2003). In total, the dataset used for our phylogenetic analysis included 15000 sequences from the small subunit rRNA gene from prokaryotic (~14000 sequences) and eukaryotic (~1000 sequences) organisms. For the more detailed analysis of the position of *Pirsonia* and *Pseudopirsonia* among the eukaryotes, 162 sequences from eukaryotic small subunit rRNA genes were used. To exclude highly variable alignment positions from the analysis, a 50% base frequency filter was constructed for the *Pirsonia* and *Pseudopirsonia* sequences, excluding positions where less than 50% of the sequences had the same nucleotide. This filter resulted in 1807 valid columns out of the 6700 alignment positions. It was applied for all different analysis methods used for the 162 sequences data set described below. In addition to the filter, correction algorithms were used to account for possible multiple substitutions (Jukes-Cantor Correction, Jukes and Cantor 1969) and branch attraction (Felsenstein correction, Felsenstein 1978). Multiple substitutions are expected to occur mainly in highly variable positions and should therefore in the analysis carried out here be already mainly excluded by the 50% base frequency filter. Tree topologies were calculated with and without the 50% base frequency filter and with and without the different correction models and resulting trees compared.

Distance analysis of the sequences was carried out using the Neighbour Joining (NJ) algorithm as implemented into the ARB software package (based on the algorithms described by Saitou and Nei (1987)) and as given in the Phylip package (J. Felsenstein, University of Washington, Phylip 3.5 and 3.6). Additionally, Maximum Parsimony (MP) and Maximum Likelihood (ML) analyses were carried out on the same dataset as used for the NJ analysis, to compare different evolutionary models. The MP method used was based on the PhylipDNA-Pars program (Version3.5c by J. Felsenstein, Copyright 1986-1993), as implemented in the ARB software. For ML calculations, the fastDNAml tool (version 1.2) was used as given in ARB and described by Olsen et al. (1994) and Felsenstein (1981). The comparison of the resulting tree topologies of all different algorithm combinations showed, that the main clusters of sequences stayed constant and did not depend on the analysis algorithm or correction model used. A bootstrap analysis was performed for the NJ analysis in the Phylip package and for the MP analysis in the ARB package using 1000 replicates (Felsenstein 1985). The dendograms shown in Figure 3A and B were based on the dendogram calculated with the ML algorithm, which included 72004 trees.

To analyse the branching order within the genus *Pirsonia* a set of 10 sequences was used, including the *Pirsonia*, *Hyphochytrium catenoides* and *Rhizidiomyces apophysatus*. All unambiguously aligned positions were used for these analyses, resulting in 1835 valid columns. Bootstrapping was carried out with 1000 replicates and the NJ, MP and ML algorithms were applied as implemented in the Phylip software package (Fig. 4A–C). The dendograms shown in Figure 4A–C were calculated using the ARB software package without bootstrapping and adapted manually to the bootstrap results calculated with the Phylip software.

Probe design: A probe specific for *Pirsonia* was designed using the ARB software package and its subfunction "probe design". The suggested probe sequences were checked for specificity using the "probe match" function implemented in ARB. The probe sequences with the highest number of mismatches to non-target sequences and a location of the mismatches in the center of the probe sequence were further checked in Genbank. The probe sequence selected according to the "in-silico" results was ordered (MWG-Biotech, Germany) and DIG labelled according to the instructions of the manufacturer (DIG Oligonucleotide Tailing Kit, Boehringer Mannheim, Germany). The specificity of the probe was tested with PCR amplified SSU rRNA genes in dot blot hybridisations.

Probe labelling and dot blot hybridisation: Unlabelled probes were supplied by MWG-Biotech (Ebersberg, Germany) and labelled with DIG using the DIG Oligonucleotide Tailing Kit (Boehringer Mannheim, Germany) following the instructions of the manufacturer. Labelled probes were mixed with dot blot hybridisation buffer to a final probe concentration of approximately 0.1 pmol ml^{-1}. PCR products were denatured by heating to 95 °C for 5 to 10 min and immediately chilled on ice. For each species tested, triplicates of 1 µl PCR product were dripped onto positively charged nylon membranes (Boehringer Mannheim, Germany), air dried and cross linked to the membrane by UV radiation for 2 × 90 s. Membranes were pre-hybridised in hybridisation buffer (5 × SSC, 0.1% N-Laurylsarcosine, 0.02% SDS, 1% blocking solution) without probe for 2 to 4 h at hybridisation temperature. After that buffer was exchanged to probe-buffer mix and hybridisation carried out over night in a hybridisation oven (Appligene, Germany). Detection was carried out using the DIG detection kit and CSPD (Roche/Enzo, Germany), following the instructions

of the manufacturer. Signals were detected by exposure to X-ray films for 15 min to 4 h.

Acknowledgements

References

Beardsley C, Pernthaler J, Wosniok W, Amman R (2003) Are readily culturable bacteria in coastal North Sea waters suppressed by selective grazing mortality? Appl Environ Microbiol **69**: 2624–2630

Bulman SR, Kühn SF, Marshall JW, Schnepf E (2001) A phylogenetic analysis of the SSU rRNA from members of the Plasmodiophorida and Phagomyxida. Protist **152**: 43–51

Cavalier-Smith,T (1998) A revised six-kingdom system of life. Biol Rev **73**: 203–266

Coats DW, Park MG (2002) Parasitism of photosynthetic dinoflagellates by three strains of *Amoebophrya* (Dinophyta): parasite survival, infectivity, generation time, and host specificity. J Phycol **38**: 520–528

Cooney EW, Barr DJS, Barstow WE (1985) The ultrastructure of the zoospore of *Hyphochytrium catenoides*. Can J Bot **63**: 497–505

Díez B, Pedrós-Alió C, Massana R (2001) Study of genetic diversity of eukaryotic picoplankton in different oceanic regions by small-subunit rRNA gene cloning and sequencing. Appl Environm Microbiol **67**: 2932–2941

Doyle JJ, Doyle JL (1990) Isolation of plant DNA from fresh tissue. Focus **12**: 13–15

Drebes G (1966) Ein parasitischer Phycomycet (Lagenidiales) in *Coscinodiscus*. Helgoländer wiss Meeresunters **13**: 426–435

Drebes G, Schnepf E (1988) *Paulsenella* Chatton (Dinophyta), ectoparasites of marine diatoms: development and taxonomy. Helgoländer Meeresunters **42**: 563–581

Drebes G, Schnepf E (1998) *Gyrodinium undulans* Hulburt, a marine dinoflagellate feeding on the bloom-forming diatom *Odontella aurita*, and on copepod and rotifer eggs. Helgoländer Meeresunters **52**: 1–14

Felsenstein J (1978) Cases in which parsimony and compatibility methods will be positively misleading. Syst Zool **27**: 27–33

Felsenstein J (1981) Evolutionary trees from DNA sequences: A maximum likelihood approach. J Mol Evol **17**: 368–376

Felsenstein J (1985) Confidence limits on phylogenies: an approach using the bootstrap. Evolution **39**: 783–791

Fuller MS (1990) Hyphochytriomycota. In Margulis L, Corliss JO, Melkonian M, Chapman DJ (eds) Handbook of Protoctista. Jones and Bartlett, Boston, pp 380–387

Grahame ES (1976) The occurrence of *Lagenisma coscinodisci* in *Palmeria hardmaniana* from Kingston Harbour, Jamaica. Br phycol J **11**: 57–61

Gunderson HJ, John SA, Boman WC, Coats DW (2002) Multiple strains of the parasitic dinoflagellate *Amoebophrya* exist in Chesapeake Bay. J Eukaryot Microbiol **49**: 469–474

Hall TA (1999) T. A. Hall. BioEdit: a user-friendly biological sequence alignement editor and analysis program for Windows 95/98/NT. Nucleic Acids Symposium Series **41**: 95–98

Janson S, Gisselson L-Å, Salomon PS, Granéli E (2000) Evidence for multiple species within the endoparasitic dinoflagellate *Amoebophrya ceratii* as based on 18S rRNA gene-sequence analysis. Parasitol Res **86**: 929–933

Jukes TH, Cantor CR (1969) Evolution of Protein Molecules. In Munro HN (ed) Mammalian Protein Metabolism. Academic Press, New York, pp 21–132

Karpov SA (1997) Cercomonads and their relationship to the myxomycetes. Arch Protistenkd **148**: 297-307

Kühn SF, Drebes G, Schnepf E (1996) Five new species of the nanoflagellate *Pirsonia* in the German Bight, North Sea, feeding on planktic diatoms. Helgoländer Meeresunters **50**: 205–222

Kühn SF, Lange M, Medlin LK (2000) Phylogenetic position of *Cryothecomonas* inferred from nuclear-encoded small subunit ribosomal RNA. Protist **151**: 337–345

Ludwig W, Strunk O, Westram R, Richter L, Meier H, Yadhukumar A, Buchner A, Gerber S, Ginhart AW, Gross S, Grunmann S, Hermann S, Jost R, König A, Liss T, May M, Reichel B, Strehlow R, Stamatakis AP, Stuckmann N, Vilbig A, Lenke M, Ludwig T, Bode A, Schleifer K-H (in press) ARB: A software environment for sequence data. Nucleic Acids Research

MacDonald CM, Darbyshire JF, Ogden CC (1977) The morphology of a common soil flagellate, *Heteromita globosa* STEIN (Mastigophorea: Protozoa). Bull Brit Mus (Natur Hist) Zool **31**: 255–264

Massana R, Guillou L, Díez B, Pedrós-Alió C (2002) Unveiling the organisms behind novel eukaryotic ribosomal DNA sequences from the ocean. Appl Environ Microbiol **68**: 4554–4558

Medlin LK, Elwood HJ, Stickel S, Sogin ML (1988) The characterization of enzymatically amplified eukaryotic 16S-like rRNA-coding regions. Gene **71**: 491–499

Moon-van der Staay S-Y, de Wachter R, Vaulot D (2003) Oceanic 18S rDNA sequences from picoplankton reveal unsuspected eukaryotic diversity. Nature **409**: 607–610

Norén F, Moestrup O, Rehnstam-Holm AS (1999) *Parvilucifera infectans* Norén et Moestrup gen. et sp. nov. (Perkinsozoa phylum nov.): a parasitic flagellate capable of killing toxic microalgae. Europ J Protistol **35**: 233–254

Olsen G J, Matsuda H, Hagstrom R, and Overbeek R (1994) fastDNAml: A tool for construction of phylogenetic trees of DNA sequences using maximum likelihood. Comput Appl Biosci **10**: 41–48

Patterson DJ (1989) Stramenopiles: Chromophytes from a Protistan Perspective. In Green JC, Landbeater BSC, Divers WL (eds) The Chromophyte Algae: Problems and Perspectives. Clarendon, Oxford, pp 357–379

Saitou N, Nei M (1987) The neighbor-joining method: a new method for reconstructing phylogenetic trees. Mol Biol Evol **4**: 406–425

Schnepf E (1994) Light and electron microscopical observations in *Rhynchopus coscinodiscivorus* sp.nov., a colourless, phagotrophic euglenozoon with concealed flagella. Arch Protistenkd **144**: 63–74

Schnepf E, Drebes G, Elbrächter M (1990) *Pirsonia guinardiae*, gen. et spec. nov.: A parasitic flagellate on the marine diatom *Guinardia flaccida* with an unusual mode of food uptake. Helgoländer Meeresunters **44**: 275–293

Schnepf E, Kühn SF (2000) Food uptake and fine structure of *Cryothecomonas longipes* spec. nov., a marine nanoflagellate incertae sedis feeding phagotrophically on large diatoms. Helgol Mar Res **54**: 18–32

Schnepf E, Schweikert M (1996) *Pirsonia*, phagotrophic nanoflagellates incertae sedis, feeding on marine diatoms: attachment, fine structure and taxonomy. Arch Protistenkd **147**: 361–371

Schweikert M, Schnepf E (1996) *Pseudaphelidium drebesii*, gen. et sp. nov. (incerta sedis), a parasite of the marine centric diatom *Thalassiosira punctigera*. Arch Protistenkd **147**: 11–17

Schweikert M, Schnepf E (1997) Light and electron microspical observations on *Pirsonia punctigerae* spec. nov., a nanoflagellate feeding on the marine centric diatom *Thalassiosira punctigera*. Europ J Protistol **33**: 168–177

Sparrow jr. FK (1960) Aquatic Phycomycetes (2nd ed) Ann Arbor, The University of Michigan Press

Tillmann U, Hesse K-J, Tillmann A (1999) Large-scale parasitic infection of diatoms in the Northfrisian Wadden Sea. J Sea Res **42**: 255–261

Thomsen HA, Bolt PA, Garrison DI (1991) Fine structure and biology of *Cryothecomonas* gen. nov. (Protista incerta sedis) from ice biota. Can J Zool **69**: 1048–1070